
Journal of Computer-Aided Materials Design, **6:** 175–183, 1999.
KLUWER/ESCOM

Kinetic Monte Carlo method for dislocation glide in silicon

WEI CAI[a,*], VASILY V. BULATOV[b] and SIDNEY YIP[a]
[a]*Department of Nuclear Engineering, Massachusetts Institute of Technology, Cambridge, MA 02139, U.S.A.*
[b]*Lawrence Livermore National Laboratory, University of California, Livermore, CA 94550, U.S.A.*

Received 27 September 1999; Accepted 27 September 1999

Abstract. A kinetic Monte Carlo (KMC) approach to the mesoscale simulation of dislocation glide via the kink mechanism is developed. In this paper we present the details of the KMC methodology, highlighting three features: (1) inclusion of dislocation dissociation; (2) efficient method of sampling the double-kink nucleation process; and (3) exact calculation of dislocation segment interactions.

Keywords: Double-kink, Kinetic Monte Carlo, Partial dislocation, Si

1. Introduction

We formulate a stochastic method of simulating the glide mobility of a single dislocation based on the sequence of elementary processes of double-kink nucleation, kink migration, and kink annihilation. The method is applied to study the coupling effect of the dissociated partial dislocations in Si. Since the inputs to the method can be obtained from atomistic calculations, the present approach constitutes a link between the atomistic events taking place on the angstrom scale with experimental observations on the micron scale.

In the case of studying atomic modes of dislocation mobility in Si, much information has been obtained using empirical interatomic potential functions [1] and the more rigorous electronic structure calculations [2] concerning the activation energies for kink nucleation and migration. However, such results have not been put to use at the mesoscale level to analyze dislocation motion measured experimentally. It is convenient to represent dislocation velocity measurements by an Arrhenius expression with an activation energy for the temperature dependence and a pre-exponential factor for the stress dependence. While this enables one to extract parameter values for the activation energy and stress exponent, this type of analysis gives little insight into physical mechanisms, and cannot make a quantitative connection with the atomistic approach.

In view of the high Peierls barrier in Si, the processes of double-kink nucleation, kink migration and kink annihilation can be regarded as rare events, their rates of occurrence being determined by the free energy barriers through the transition state theory [3]. If all the activation energies can be obtained from atomistic calculations, a kinetic Monte Carlo (KMC) simulation [4] then can be developed to sample the overall configurational space of dislocation motion, and thus predict the dislocation velocity [5]. Recently a lattice-based kinetic Monte Carlo method has been introduced to study general aspects of finite size effects in dislocation dynamics [6].

*To whom correspondence should be addressed. E-mail: caiwei@mit.edu

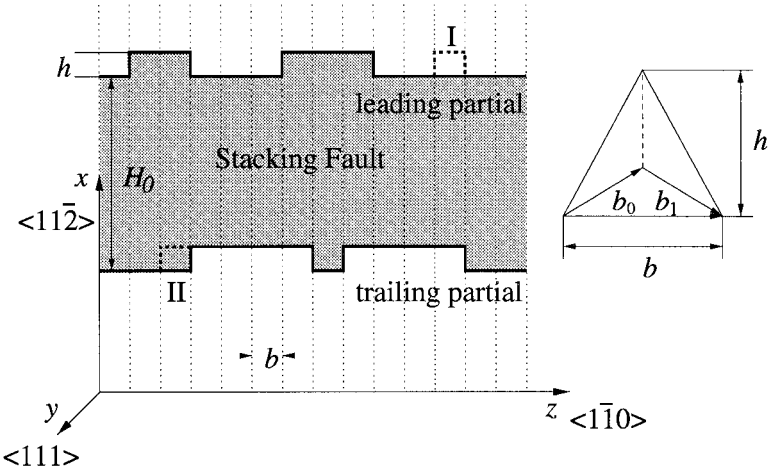

Figure 1. Schematic representation of dislocation in Si in the KMC simulation. Screw dislocation with Burgers vector $\vec{b}$ is dissociated into leading and trailing 30° partials, with Burgers vectors $\vec{b}_0$ and $\vec{b}_1$ respectively. The elementary kink width is b. The kink height is $h = \sqrt{3}/2\, b$. An embryonic double-kink nucleation event is shown at position I, and a kink migration event is shown at position II, both in dashed lines.

In this paper we give a detailed formulation of a KMC model of the glide motion of a dissociated dislocation in Si at arbitrary temperature and applied stress. The description is based on the following conditions. The dislocation is dissociated into two partials which are connected by a stacking fault [7]. While each partial moves by the process of kink nucleation and migration, where the respective activation energies will be given by atomistic calculations, the effects of the stacking fault and Peach Koehler interactions also need to be taken into account. It is clear that the description being developed here incorporates much more mechanistic details than the well-known Hirth–Lothe model for dislocation glide [8]. On the other hand, we have intentionally neglected the effect of kink multiplicities [9] for the sake of simplicity, reserving this issue for future studies.

2. Simulation methodology

2.1. General settings

We show in Fig. 1 a schematic description of the dislocation model which we analyze. The dissociated dislocation moving in the upward ($+x$) direction consists of two piecewise linear lines, each representing a partial dislocation composed of horizontal (H) and vertical (V) segments. H segments have a length in multiple of b and the V segments have length h, the kink height. The area enclosed by the two partials (shaded) is the stacking fault, whose width is always a multiple of h. Each partial can migrate upward or downward through a series of segmental events. On the H-segment one can have double-kink nucleation in the upward or downward directions, while the V-segment can migrate to the left or right (indicated by the dashed lines).

In this work, we study a screw dislocation dissociated into two 30° partials, with the xz plane being the glide plane. Periodic boundary conditions are applied in the z direction so that the dislocation lines have no ends. Initially both partials are straight. This means that during the simulation, the number of left kinks and right kinks on each partial must remain identical.

For simplicity, we ignore the kink multiplicity [9] in this work; the formation energies E_k and migration barriers W_m for all the kinks are taken to be the same.

The totality of the positions z_i and senses v_i ($+1$ or -1 for left or right) of all kinks, together with H_0, the partial separation at $z = 0$, completely specify the geometry of the dislocation. We refer to it as the *system configuration*.

The simulation proceeds by following the evolution of the system configuration as a consequence of the occurrence of a certain sequence of elementary events. These are double-kink nucleations, kink migrations, and kink annihilations, and they occur in competition with each other. At every Monte Carlo step, all the possible events are considered but only one is selected to occur; the reciprocal of the sum of the rates of all the possible events considered then determines the real time duration of the step.

Now we start to calculate the rates of the elementary events. Consider the energy costs of a double-kink nucleation process in the configuration depicted in Fig. 1 in the presence of an external stress. First one has the activation energy for formation of an embryonic double kink E_{emb}. By embryonic we mean the kink width is $1b$. Second, one has an energy bias due to the presence of the stacking fault which favors reduction of the stacking fault area (see Fig. 1). In fact, this bias makes it more likely to nucleate a double-kink downward on the leading partial and double-kink upward on the trailing partial. Last, there is the interaction between the current segment and the local stress field which includes the effects of the applied stress and stresses due to all the other segments. In view of these three components the occurrence rate of double-kink nucleation, H-segment activity, is given by

$$j_{dk}(1) = \omega_0 \exp\left(-\frac{E_{emb} - TS + (E_{SF} - \vec{\tau}\cdot\vec{b}_\alpha)A/2}{k_B T}\right), \tag{1}$$

where ω_0 is an attempt frequency factor, which we will set equal to the *Debye frequency* of Si in this work. The term $-TS$ is to account for the vibrational entropy contribution of the saddle point of this transition. $E_{SF} = \pm\gamma_{SF}$, γ_{SF} being the stacking fault energy, with the '$+$' and '$-$' signs for leading and trailing partial, respectively. $\vec{\tau}$ is a vector in the xz plane defined through the components of the stress tensor σ as $\vec{\tau} = (\sigma_{yz}, \sigma_{xy})$. $\vec{b}_\alpha$ are the Burgers vectors, with $\alpha = 0, 1$ for the leading and trailing partials, respectively, $\vec{b}_0 = (b/2, b\sqrt{3}/6)$ and $\vec{b}_1 = (b/2, -b\sqrt{3}/6)$. $A = \pm bh$ is the area swept out by the dislocation as a result of kink nucleation in the upward ($+$) and downward ($-$) directions, respectively. k_B is Boltzmann's constant and T is the temperature.

The factor of $1/2$ appears in Equation 1 because we assume that the dislocation has swept out half of the total area A at the saddle point configuration. This assumption is valid for the small stresses, where the work done by the stress is much smaller than the energy barrier itself. In this paper the criterion becomes $\tau \ll E_{emb}/b^3$ and simple calculations show that it is satisfied in the normal range of stresses.

For kink migration, the V-segment activity, the corresponding rate j_m involves the same energy contributions as in j_{dk} except that E_{emb} is replaced by the kink migration barrier W_m. Kinks may annihilate as a result of their migration. So we do not calculate the kink annihilation rate separately.

At the beginning of each step, an *event list* of all the *possible* events is generated from the current system configuration. We calculate the rates of all the events in the list, including double-kink nucleations, kink migrations and kink annihilations. A standard Monte Carlo move is made by choosing a particular event from the list with a probability that is propor-

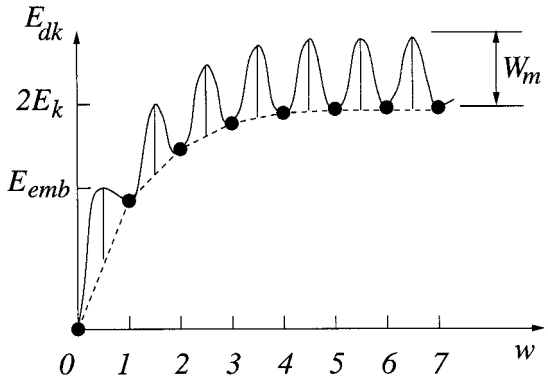

Figure 2. Theoretical dependence of the kink pair energy E_{dk} on its width w, shown as dots. For large width it approaches $2E_k$. At finite width w, E_{dk} is a superposition of $2E_k$ and the kink pair interaction energy $W_{int}(w)$. The solid curve illustrates the energy barrier between the neighboring states. E_{emb} is the barrier for nucleating an embryonic double-kink, i.e. transition from state $w = 0$ to $w = 1$.

tional to its occurrence rate [10]. The system takes a new configuration after the move and the procedure repeats itself. The physical time elapsed for this step is the inverse of the total rate of all the possible events in the event list.

2.2. Treatment of double-kink nucleation

Two aspects of simulating the process of double-kink nucleation in the present method deserve further attention. One is that we need to specify the value of E_{emb} for nucleating an embryonic double-kink. Our problem is to relate this quantity to the results of atomistic simulations, in which one calculates the single kink formation energy E_k and kink migration barrier W_m.

We plot in Fig. 2 the profile of an energy E_{dk} showing the variation of the double-kink energy with its width w. For large width this quantity approaches $2E_k$. At finite width w, $E_{dk}(w)$ is a superposition of $2E_k$ and the interaction energy W_{int} between the kink pair, as indicated by the dots in Fig. 2. From linear elastic theory we have [8]:

$$E_{dk}(w) = 2E_k + W_{int}(w), \ (w \geq 1) \tag{2}$$

$$W_{int}(w) = -\frac{\mu h^2}{8\pi w b}\left(b_z^2\frac{1+\nu}{1-\nu} + b_x^2\frac{1-2\nu}{1-\nu}\right), \tag{3}$$

where $b_z = b/2, \ b_x = b\sqrt{3}/6$.

Given that W_m is the energy barrier separating two neighboring states of the double-kink in the limit of large width (c.f. Fig. 2), we will assume that at finite width including a width of one b, the barrier between adjacent states is still given by placing W_m at the midpoint between the two states. This leads to the following expressions for the transition barriers of each state

$$W^+(i) = \frac{1}{2}[E_{dk}(i+1) - E_{dk}(i)] + W_m, \tag{4}$$

$$W^-(i) = \frac{1}{2}[E_{dk}(i-1) - E_{dk}(i)] + W_m, \tag{5}$$

where $W^+(i)$ and $W^-(i)$ are the energy barriers for the forward ($i \to i+1$) and backward ($i \to i-1$) transitions respectively. Specifically, for a width of one b we obtain

$$E_{emb} = W^+(0) = \frac{1}{2}[2E_k + W_{int}(1)] + W_m. \tag{6}$$

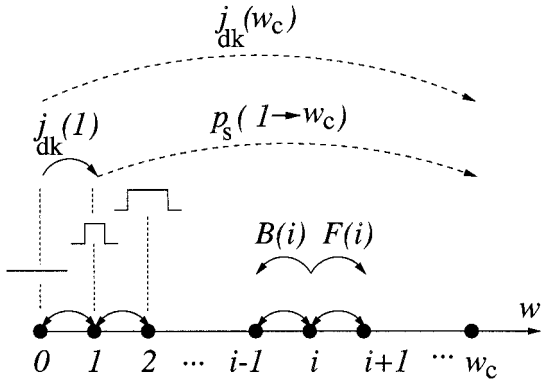

Figure 3. Schematic representation of the Markov process in the space of discrete kink width w. Transitions are allowed between neighboring states, shown as solid arcs. Every state can be reached from every other state. We draw dashed arcs between states widely separated to denote a collection of different paths. $F(i)$ and $B(i)$ are the forward and backward probabilities from state i. The nucleation rate $j_{dk}(w_c)$ of double-kinks of width w_c is the product of embryonic double nucleation rate $j_{dk}(1)$ with the survival rate $p_s(1 \rightarrow w_c)$.

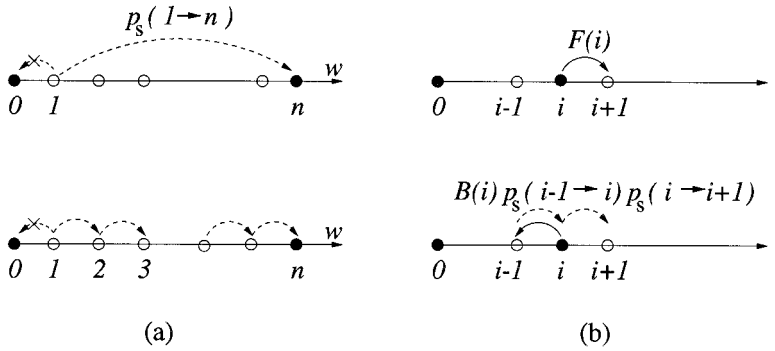

Figure 4. (a) Survival probabilities $p_s(1 \rightarrow n)$ can be broken up as the multiplication of smaller survival probabilities $p_s(i \rightarrow i+1)$. (b) Two possibilities of reaching $i+1$ from i. First, it can jump to $i+1$ directly in the first step. Second, it can jump to $i-1$ in the first step. But then it has to come back to i from $i-1$ before it can reach $i+1$.

The second aspect of simulating the double-kink nucleation concerns efficiency. A direct simulation taking into account embryonic double-kink nucleation, as described above, would be very inefficient because most embryonic kink pairs have a large tendency to annihilate among themselves, which will not contribute to the overall dislocation motion. This problem is solved by specifying in the simulation procedure that double-kink nucleation occurs only with a width w_c. The proper choice of w_c involves compromising between two constraints, a large value of w_c to make the simulation proceed faster and a small value to describe more accurately the expansion of kink pair. For present calculations we have adopted somewhat arbitrarily a value of $w_c = 10$; we have found that the results are not very sensitive to a variation in this w_c value by a factor of 2.

Given the choice of w_c we need to calculate the nucleation rate of a double-kink of width w_c. We write

$$j_{dk}(w_c) = j_{dk}(1) \cdot p_s(1 \rightarrow w_c), \tag{7}$$

where $j_{dk}(1)$ is the embryonic double-kink nucleation rate defined in Equation 1 and p_s is the *survival probability* that an embryonic double-kink successfully reaches a width w_c before it is annihilated.

More rigorously, we define p_s as follows. Consider the double-kink nucleation and expansion process as a Markov process in the discrete space of kink width w, $w = 0, 1, 2, \cdots$, see Fig. 3. The state $w = 0$ corresponds to the situation where there is no kink pair. Then $p_s(i \rightarrow n)$ is the probability of reaching state n by starting from state i without ever reaching state 0. The condition of $i < n$ is always assumed.

Because of the connectivity of the 1D Markov chain, we observe that starting from state 1, the system has to reach $n-1$ before n, and it has to reach $n-2$ before it reaches $n-1$, and so on. Therefore, we can express the survival probability $p_s(1 \rightarrow n)$ as the product of the elementary ones, see Fig. 4a.

$$p_s(1 \rightarrow n) = \prod_{i=1}^{n-1} p_s(i \rightarrow i+1). \tag{8}$$

To evaluate $p_s(i \rightarrow i+1)$, we note that there are two possibilities of reaching $i+1$ from i, as shown in Fig. 4b. First, the system can go to $i+1$ upon the first jump from state i. That has the probability of $F(i)$, which we will give explicit expression below. Second, the system can choose to go to $i-1$ upon the first jump from i. This has the probability of $B(i) = 1 - F(i)$. Since it makes the 'wrong' move in its first step, it has to correct itself sometime later by coming back to i before it can reach $i+1$. The probability of coming back to i from $i-1$ is $p_s(i-1 \rightarrow i)$. After that, the situation is exactly the same as the initial stage, when the system starts off from state i. The probability of reaching $i+1$ now is $p_s(i \rightarrow i+1)$ again. Therefore we have the recursive equation

$$p_s(i \rightarrow i+1) = F(i) + B(i)p_s(i-1 \rightarrow i)p_s(i \rightarrow i+1). \tag{9}$$

Solving for $p_s(i \rightarrow i+1)$ in terms of $p_s(i-1 \rightarrow i)$ we have:

$$p_s(i \rightarrow i+1) = \frac{F(i)}{1 - B(i)p_s(i-1 \rightarrow i)}, i \geq 1. \tag{10}$$

With the initial condition of $p_s(0 \rightarrow 1) = 0$ we can solve for $p_s(i \rightarrow i+1)$ for all $i = 1, \cdots, n$. The $F(i)$ in Equations 9 and 10 is defined as the *forward probability* of state i – the probability of going to $i+1$ instead of $i-1$ upon leaving i. $B(i)$ is defined as the *backward probability* which is just $1 - F(i)$. In terms of the transition barriers given in Equations 4 and 5, the expression for $F(i)$ is

$$F(i) = \left[1 + \exp\left(\frac{W^+(i) - W^-(i)}{k_B T}\right)\right]^{-1}, \; i \geq 1, \tag{11}$$

where $W^+(i)$ and $W^-(i)$ are the transition barriers given in Equations 4 and 5. At finite stress and in the presence of the stacking fault, the expression of $F(i)$ becomes

$$F(i) = \left[1 + \exp\left(\frac{W^+(i) - W^-(i) - (E_{SF} - \vec{\tau} \cdot \vec{b}_\alpha)A}{k_B T}\right)\right]^{-1}, \tag{12}$$

where the additional terms have the same meaning as in Equation 1. The rate $j_{dk}(w_c)$ of nucleating double-kink of width w_c is now fully specified in Equations 1 through 12.

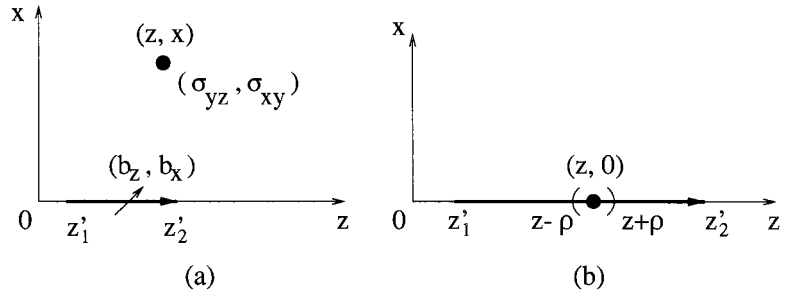

Figure 5. Stress calculation of dislocation segment for the points on the glide plane.

2.3. STRESS CALCULATION

The explicit form of the stress of a straight dislocation segment at a given point is given in Reference 8. In this work, where the dislocation is confined to the xz plane, the results are greatly simplified. For a configuration shown in Fig. 5, $\sigma_{xy} = \sigma_{xy}(z_2') - \sigma_{xy}(z_1')$ and $\sigma_{yz} = \sigma_{yz}(z_2') - \sigma_{yz}(z_1')$.

$$\frac{\sigma_{xy}(z')}{\sigma_0} = \begin{cases} -b_x \frac{x}{R(R+\lambda)} & z < z_1' < z_2' \\ b_x \frac{\lambda}{xR} & z_1' < z < z_2' \\ b_x \frac{x}{R(R-\lambda)} & z_1' < z_2' < z \end{cases} \tag{13}$$

$$\frac{\sigma_{yz}(z')}{\sigma_0} = \begin{cases} \nu b_x \frac{1}{R} - (1-\nu)\frac{b_z x}{R(R+\lambda)} & z < z_1' < z_2' \\ \nu b_x \frac{1}{R} + (1-\nu)\frac{b_z \lambda}{xR} & z_1' < z < z_2' \\ \nu b_x \frac{1}{R} + (1-\nu)\frac{b_z x}{R(R-\lambda)} & z < z_1' < z_2' \end{cases} \tag{14}$$

Here $\sigma_0 = \mu/4\pi(1-\nu)$ and $\lambda = z' - z$, $R^2 = x^2 + (z-z')^2$. Note that three forms are used to evaluate stress in three different situations to ensure numerical stability.

To calculate the stress at a point on the dislocation segment, as shown in Fig. 5b, we use the 'principal value'. This is to say, we attribute the stress at point $(z, 0)$ due to the segment z_1', z_2' as the superposition of the stress due to two segments $z_1', z-\rho$ and $z+\rho, z_2'$, and take the limit of $\rho \to 0$. Specifically, when $x = 0$, $z_1' < z < z_2'$, we have $\sigma_{xy} = 0$ and $\sigma_{yz} = \sigma_{yz}(z_2') - \sigma_{yz}(z_1')$, with

$$\frac{\sigma_{yz}(z')}{\sigma_0} = \nu b_x \frac{1}{R}. \tag{15}$$

After a kinetic Monte Carlo step, the stress at every point of interest changes due to the event which just occurred – a double-kink nucleation, a kink migration or a kink pair annihilation. The corresponding stress change can always be evaluated as a stress field of a rectangular dislocation loop. We keep track of the stress field by updating the stress change after each KMC step.

3. Results

Figure 6 shows the evolution of the profile for the leading partial of a moving screw dislocation. The simulation is carried out at a resolved shear stress of $\sigma_{yz} = 50$ MPa and a temperature

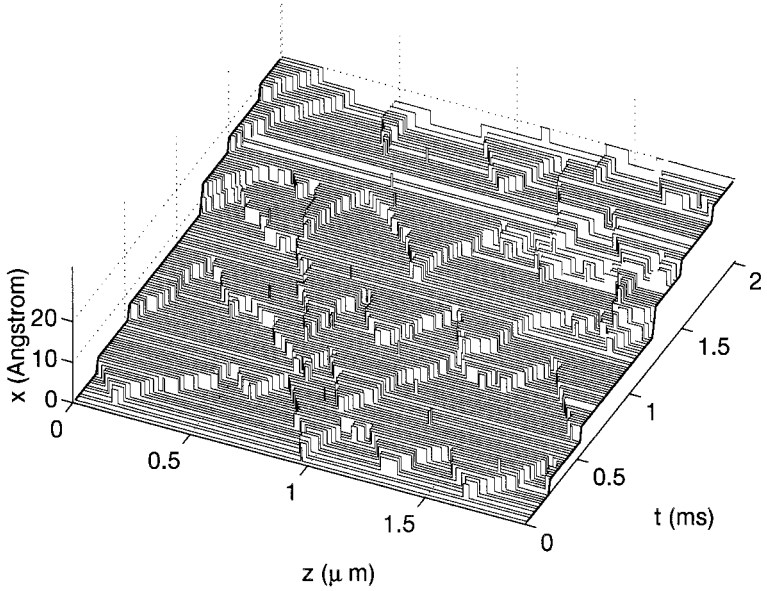

Figure 6. Profile of the leading 30° partial dislocation during the motion at $T = 1000$ K, $\sigma_{yz} = 50$ MPa. The dislocation length is $5000b = 1.92\ \mu m$. Periodic boundary conditions are applied. Energy parameters used are $E_k = 0.52$eV, $W_m = 0.89$ eV.

of $T = 1000$ K. The energy parameters we use are $E_k = 0.52$ eV, $W_m = 0.89$ eV, which are based on the atomistic calculations of the EDIP [11] potential for Si. The vibrational entropy in Equation 1 is set to $S = 3k_B$, according to some theoretical and experimental estimations [12,13]. The stacking fault energy is chosen to be $\gamma_{SF} = 0.004$ eV/Å^2, so that the separation between the two partials is around $10h$.

The simulation starts at $t = 0$ with a straight dislocation. Shortly after, a double-kink is nucleated in the middle of the dislocation. The two kinks begin to drift in opposite directions and finally annihilate with neighboring kinks. As more double-kinks are nucleated and more kink pairs annihilated, the system reaches a steady state, with about 10 kinks on the 2 μm long dislocation at any instant. At $t = 2$ ms, the dislocation has glided a distance of 6 kink heights in the x direction, which is about 20 Å. For a detailed discussion of the choice of energy parameters and more simulation results, the reader is referred to [14].

4. Concluding remarks

We have formulated a kinetic Monte Carlo model capable of describing the planar glide of a dissociated dislocation in Si in a thermal environment with the presence of an applied stress. Full implementation details are discussed in the context of an efficient method of sampling double-kink nucleation. First results, showing how individual kinks nucleate, migrate, and annihilate during the evolution of a 30° partial on the mesoscale of length and time, are presented. The model can be used to predict dislocation velocity as a function of temperature and applied stress, results that can be directly compared with experiment [15].

The present approach is applicable to single dislocation motion. To treat the kinetic behavior of an assembly of dislocations, the method of dislocation dynamics has been developed [16]; a current challenge parallel to what we have encountered here is to link the

atomistic calculation with this powerful method of dealing with dislocation interactions [17, 18].

Acknowledgements

This work was initially supported by the MIT MRSEC Program of the National Science Foundation under award number DMR 94-00334, and later by the Lawrence Livermore National Laboratory through the DOE ASCI-level II program.

References

1. Bulatov, V.V., Yip, S. and Argon, A.S., Phil. Mag. A, 72 (1995) 453.
2. Nunes, R.W., Bennetto, J. and Vanderbilt, D., Phys. Rev. Lett., 77 (1996) 1516.
3. Glasstone, S., Laidler, K.J. and Eyring, H., The Theory of Rate Processes, McGraw-Hill, New York, NY, 1941.
4. Binder, K., Monte Carlo Methods in Statistical Physics, 4th ed., Springer-Verlag, Berlin, 1979, p. 12.
5. Cai, W., Bulatov, V.V., Justo, J.F., Yip, S. and Argon, A.S., Mater. Res. Soc. Proc., 538 (1999) 69.
6. Lin, K. and Chrzan, D.C., Phys. Rev. B, 60 (1999) 3799.
7. Möller, H.J., Acta. Metall., 26 (1978) 963.
8. Hirth, J.P. and Lothe, J., Theory of Dislocations, Wiley, New York, NY, 1982.
9. Bulatov, V.V., Justo, J.F., Cai, W. and Yip, S., Phys. Rev. Lett., 79 (1997) 5042.
10. Bortz, A.B., Kalos, M.H. and Lebowitz, J.L., J. Comput. Phys., 17 (1975) 10.
11. Justo, J.F., Bazant, M.Z., Kaxiras, E., Bulatov, V.V. and Yip, S., Phys. Rev. B, 58 (1998) 2539.
12. Marklund, S., Solid State Commun., 54 (1985) 555.
13. Louchet, F., Phil. Mag. A, 43 (1981) 1289.
14. Cai, W., Bulatov, V.V., Justo, J.F., Argon, A.S. and Yip, S., to be published.
15. George, A., J. Phys. (Paris), C6 (1979) 40.
16. Devincre, B. and Kubin, L., Mater. Sci. Eng., A8 (1997) 234.
17. Bulatov, V.V., Abraham, F.F., Kubin, L., Devincre, B. and Yip, S., Nature, 391 (1998) 669.
18. Bulatov, V.V. and Kubin, L.P., Curr. Opin. Solid State Mater. Sci., 3 (1998) 558.